

**KERNFORSCHUNGSZENTRUM**

**KARLSRUHE**

Oktober 1973

KFK 2109

Institut für Angewandte Kernphysik

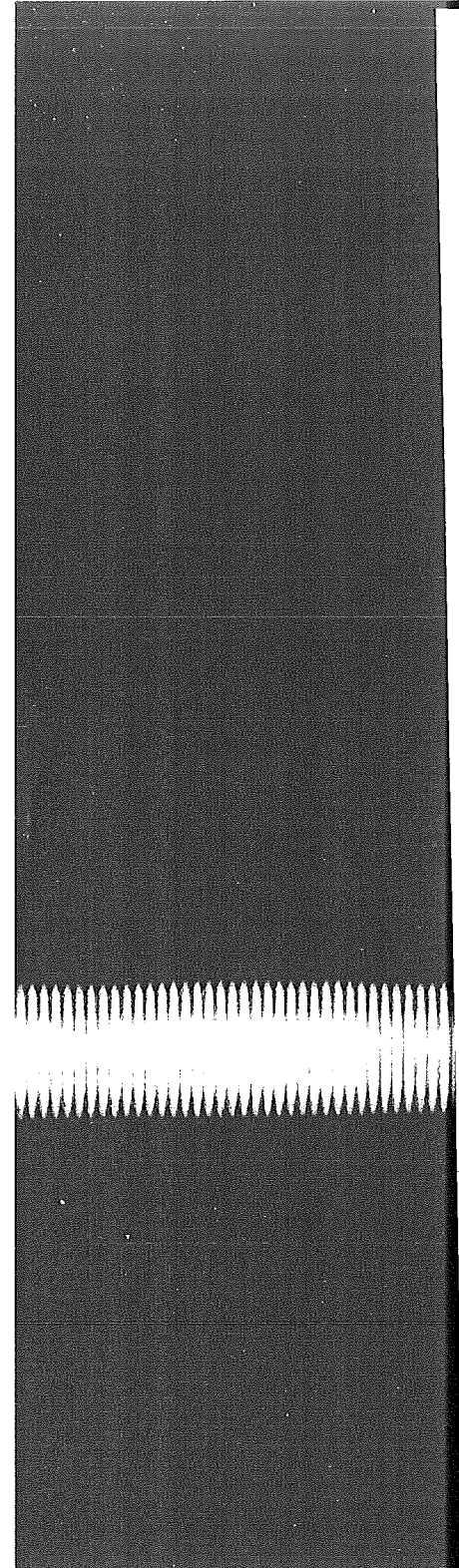
**Radiation Damage and Ion Behaviour in Ion Implanted Vanadium  
and Nickel Single Crystals;  
Ion Implantation in Superconducting Thin Films**

M. Gettings, K.G. Langguth, G. Linker  
O. Meyer, H. Mann, E. Phrlingos



**GESELLSCHAFT  
FÜR  
KERNFORSCHUNG M.B.H.**

**KARLSRUHE**



Als Manuskript vervielfältigt  
Für diesen Bericht behalten wir uns alle Rechte v

GESELLSCHAFT FÜR KERNFORSCHUNG M  
KARLSRUHE

RADIATION DAMAGE AND ION BEHAVIOUR IN ION IMPLANTED VANADIUM AND  
NICKEL SINGLE CRYSTALS

M. Gettings, K.G. Langguth and G. Linker

Institut für Angewandte Kernphysik

Kernforschungszentrum Karlsruhe

ABSTRACT

Distributions and annealing behaviour of heavy ion induced radiation damage in single crystal nickel and vanadium are compared. Sharp annealing stages are reported for Ni while for V the production of a polycrystalline layer, ascribed to the action of precipitates, prevented the annealing of damage after high dose implantations. The use of  ${}^4\text{He}^+$  ion channelling revealed disorder at depths much greater than the ions projected range, an observation that was supported by electron microscopy measurements. Implanted ion diffusion in vanadium was found to be dependent on the ion species used and the annealing behaviour of precipitates. Preliminary quantitative measurements indicate that diffusion coefficients are low.

INTRODUCTION

The investigation of radiation damage in transition metals by heavy ion bombardment is rapidly becoming a useful means of simulating long term damage in reactor environments. Further, there appears to be a growing interest in alloying and isotope enrichment using high dose implantation. In this present study, radiation damage and ion diffusion have been studied in the reactor base metals nickel and vanadium.

For fcc structured nickel, a number of electron microscopy investigations<sup>(1-3)</sup> dealing with radiation damage have been reported. At low ion doses in this metal, only vacancy clusters have been detected while for higher doses interstitial clusters are

dominant. In general, the majority of damage has been detected within the ion projected range, although in other fcc metals some interstitial clusters at depth greater than the ion ranges, have been observed and explained by focussed collision sequences<sup>(4)</sup>.

For bcc vanadium, however, only few results are presently available<sup>(5)</sup>. In previous publications<sup>(6,7)</sup> dealing with single crystal vanadium, we have reported enhanced damage depths with increasing ion energy and dose, a small dependence of the magnitude of damage on these parameters, the generation of a polycrystalline layer in the ion range for high dose implants and values of substitutional components dependent on the implanted ions ionic radii.

Results reported in this present work have been obtained using the backscattering technique from single crystal nickel implanted with bismuth, and single crystal vanadium implanted with gallium, bismuth and selenium. Some preliminary electron microscopy measurements have been taken for gallium ion induced damage in vanadium. The backscattering technique has also been employed to monitor the distribution of the implanted ions and its subsequent variations during heat treatment.

#### EXPERIMENTAL

Our backscattering system and the surface preparation of vanadium single crystals have been described in detail elsewhere<sup>(7)</sup>. Like vanadium, nickel single crystals produced by electron beam zone refining have been purchased from Metals Research Corporation. Nickel samples were cut perpendicular to the  $\langle 110 \rangle$  direction with a continuous wire saw and subsequently lapped with 15  $\mu$ , 7  $\mu$ , 1  $\mu$  and 0.25  $\mu$  diamond pastes. Samples were then etched for 5 second periods in a solution consisting of 30 cc  $\text{HNO}_3$ , 10 cc  $\text{H}_2\text{SO}_4$ , 10 cc  $\text{H}_3\text{PO}_3$  and 50 cc glacial  $\text{CH}_3\text{COOH}$  held between 85 - 95°C. Vanadium samples for our electron microscopy studies were prepared by mechanically thinning from the not implanted side to 0.1 mm by careful polishing on SiC paper followed by a vibratory polish with  $\gamma\text{-Al}_2\text{O}_3$  of 0.05  $\mu$  diameter. Final thinning was done electrolytically with a mixture of 80 % acetic acid and 20 % perchloric acid. With this technique depth determination was estimated to be about  $\pm 200 \text{ \AA}$ .

Implantations were performed at room temperature with a scanned ion beam from a heavy ion accelerator. Metal samples were bombarded over an energy range from 20 - 360 keV and a dose range of  $10^{15}$  -  $10^{17}$  ions/cm<sup>2</sup>. Irradiated specimens were annealed in a stainless steel tube under a vacuum of  $\leq 6 \times 10^{-7}$  torr, isochronally, to temperatures of 1000°C and isothermally for times lasting to 18.5 hours.

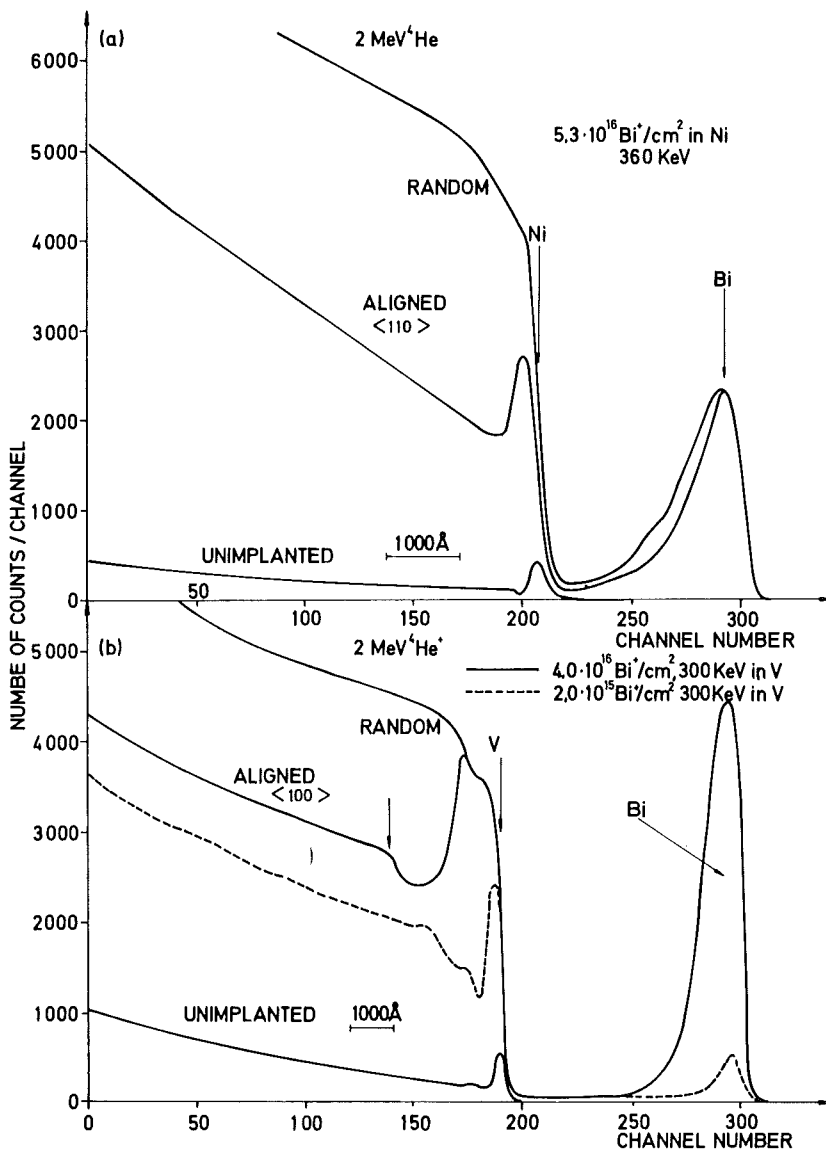


Fig. 1 Backscattering spectra from aligned and randomly oriented samples showing the damage produced in nickel and vanadium single crystals by bismuth ion bombardment.

## RESULTS

The results reported in this paper will be presented in two distinct sections:-

- a) A comparison of damage and annealing in nickel and vanadium
- b) Diffusion of implanted components in vanadium

a): In an attempt to compare radiation damage produced during ion implantation in vanadium and nickel, single crystals were bombarded with similar doses of Bi ions having the same energy. Typical aligned and random backscattering spectra from both nickel and vanadium are presented in figure 1 to show differences in the generated damage distributions. In nickel close to the surface, in a depth region between 350 and 450 Å for nonchannelled implants, a surface peak is found for all doses and energies under consideration. The area of this peak increases with ion dose and decreases with energy. In the case of channelled implantations only the deep damage has been observed. Near surface disorder in vanadium however, was found to be strongly dependent on ion dose. For doses lower than  $10^{16}$  ions/cm<sup>2</sup>, a narrow surface peak (<200 Å) was detected, whereas for higher doses a polycrystalline layer was formed over the range of the implanted ions. These surface peaks in both vanadium and nickel are thought to be disordered layers rather than oxides, as no enhanced oxygen peaks were found using the helium-oxygen resonance at 3.06 MeV <sup>4</sup>He<sup>+</sup> ion energy.

The layer produced by high dose implantations in vanadium has been investigated by X-ray diffraction and was found to be of a polycrystalline nature having the vanadium bcc structure. We ascribe this layer formation to the generation of precipitates produced when the solubility limit of Bi in vanadium is exceeded. Such precipitates are expected to partially destroy the host lattice in the region of the implanted ions. These precipitates and lattice distortions cause a backscattering rate equal to that of a randomly oriented sample. As the dechannelling from these polycrystalline layers was found to be lower than that from evaporated vanadium layers of similar thicknesses, it is concluded that the single crystal has not been completely disrupted and coherent precipitations of the implanted ions may occur.

For nickel, the absence of a polycrystalline layer is attributed to the lower concentration of bismuth ions in this material, as compared with vanadium for similar total doses. These lower concentrations and ion distribution broadening can in turn be explained by the high sputtering yields of Bi ions in nickel compared to Bi in vanadium<sup>(8)</sup>. Besides the near surface damage, damage at depths considerably greater than the ion projected range was observed in both nickel and vanadium. Differences in the struc-

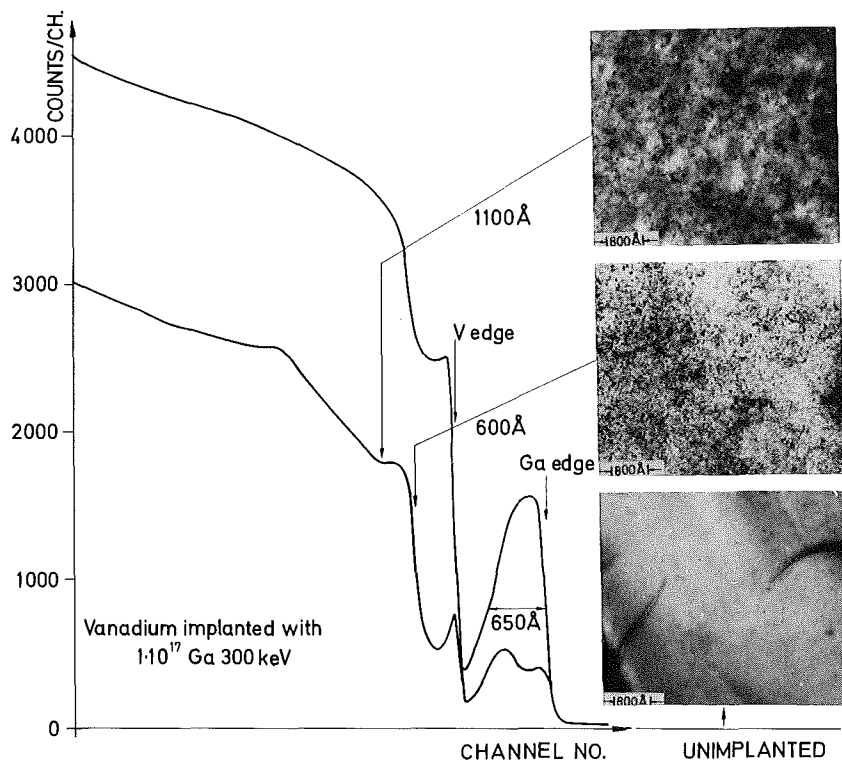


Fig. 2 Electron microscopy photographs from unimplanted and implanted ( $10^{17}$  Ga/cm<sup>2</sup>, 300 keV) vanadium samples together with a backscattering spectrum indicating the depths at which photographs were taken.

ture of this deep damage, as revealed in the backscattering spectra, were observed for the two metals investigated. For vanadium, in the absence of a polycrystalline layer, a relatively damage-free region was observed behind the surface disorder peak and a characteristic knee was evident in the disorder distribution deeper in the crystal - as indicated in figure 1(b) by the arrow. In nickel, the deep damage distribution, as observed by channelling, exhibited no structure and was manifested by a growing dechannelling rate behind the surface damage peak.

As the backscattering method does not give any information about the nature of the generated damage, preliminary electron microscopy studies have been performed to characterize the deep damage in vanadium. The results for a sample implanted with  $10^{17}$  ions/cm<sup>2</sup> of Ga are presented in figure 2 together with a backscattering spectrum indicating the two depths at which microscope photographs were taken. Also included is a picture taken with the same magnification from an unimplanted vanadium single crystal.

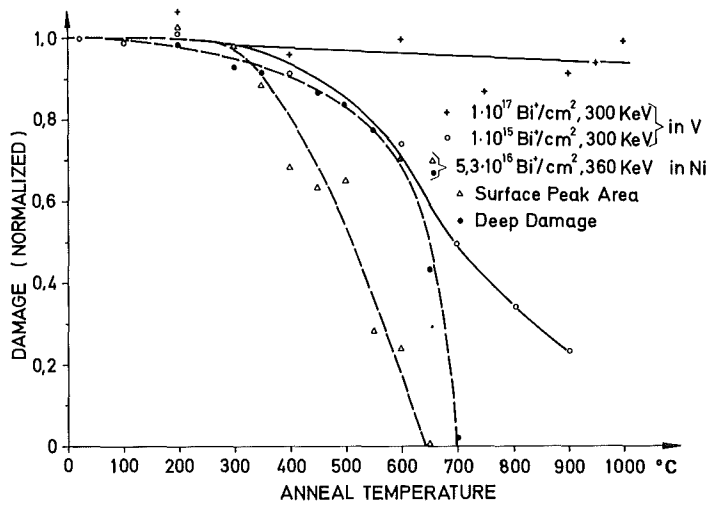


Fig. 3 Annealing curves for different types of damage generated by Bi implantations in vanadium and nickel.

At depths of 600 and 1100 Å within the crystal a fine grain structure was detected, which was observed to have more contrast at the shallower depth. At 1100 Å, voids with approximately 30 - 80 Å diameter were evident. In addition, in the diffraction patterns taken, we observed weak reflections which were attributable to small particles in a low concentration having an incoherent but ordered distribution in the host lattice. While no electron microscopy experiments have been performed for nickel in this study, others<sup>(4)</sup> have reported damage considerably beyond ion ranges. The enhanced penetration was explained by focussed collision sequences and the damage identified as interstitial clusters.

Annealing behaviour of the radiation damage in vanadium was found to be dependent on ion dose and the formation of a polycrystalline layer, whereas for nickel no such a dependence has as yet been found. These differences in annealing behaviour are illustrated in figure 3. In this figure, relative damage quantities measured by different methods are normalized to unity from samples that have not been annealed. In nickel, an annealing stage between 350° and 550°C was observed for the near surface disorder, and a stage between 500° and 700°C was found for the deep damage. Annealing of low dose vanadium implants produced, for both surface disorder and deep damage, a broad annealing stage between 500°C and 900°C. Little variation in the amount of radiation damage has been observed for the high dose implants, besides those crystals implanted with gallium, where the damage annealing is accompanied by a complete recrystallisation of the polycrystalline layer.

b): Ion behaviour in vanadium has been studied after both low and high dose implantations for several different ions. For all systems studied, implantation profiles did not exhibit a symmetrical gaussian distribution, as predicted from LSS-theory, and a deeply penetrating tail has been observed. As sputtering coefficients for vanadium are low this tail may be due to radiation enhanced diffusion. Such a process has been postulated by Smith<sup>(9)</sup> for ion implantation in metals.

With low dose implantations, where a low damage level is observed in the range of the implanted ions, mainly indiffusion of the implanted species occurred. The diffusion starts at about 900°C, although starting temperatures and diffusion rates were found to be dependent on ion species.

The ion behaviour, after high dose implantations, has been studied in some detail employing both isochronal and isothermal temperature treatments. Diffusion characteristics have been found to be dependent on the atomic radii of the implanted ions. It has been previously reported<sup>(7)</sup> that substitutional solubility levels show a strong dependence on this parameter and therefore ion species were selected to encompass diffusion mechanisms over a wide atomic radii range.

For Ga, whose atomic radius "fits best" into the vanadium lattice, diffusion from the polycrystalline layer is closely rela-

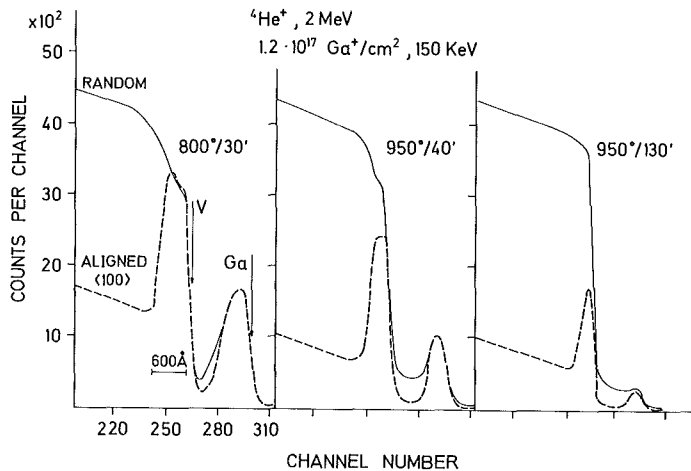


Fig. 4 Polycrystalline layer for  $1.2 \times 10^{17} \text{ Ga}^+/\text{cm}^2$  150 keV implantation and its recrystallisation, accompanied by substitutional Ga indiffusion in an isothermal annealing process.

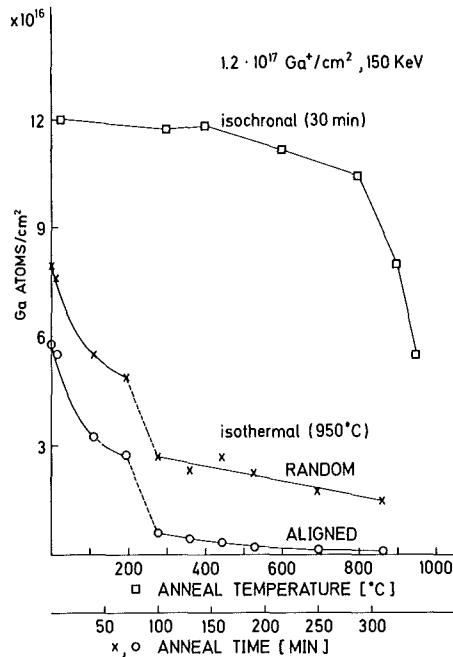


Fig. 5 Number of implanted Ga atoms/cm<sup>2</sup> remaining in vanadium as a function of temperature and time in isochronal and isothermal annealing processes showing different stages in Ga diffusion.

ted to this layer recrystallisation. Substitutional indiffusion of the Ga atoms, starting between 800 and 900°C, has been observed and backscattering spectra from this process are shown in figure 4. Here a prediffusion stage is compared with two steps in the isothermal process at 950°C. More quantitative measurements, as recorded in figure 5, reveal that the diffusion process is not uniform and three distinct stages are evident. Initially diffusion from the layer was proportional to the square root of the diffusion time. In a step between 75 and 100 minutes a rapid indiffusion occurred; it was in this period that the majority of the polycrystalline layer recrystallized. Following this rapid diffusion, little Ga movement was detected and complete reordering is accomplished after the total loss of impurity atoms.

With Se, which has a smaller atomic radius than vanadium, two distinct annealing processes were observed and are illustrated in figures 6 and 7 for a dose of  $1.2 \times 10^{17}$  Se ions/cm<sup>2</sup> implanted at an energy of 200 keV. Isochronal annealing produced little loss of the implanted constituent as can be seen in figure 6. Movement of Se was detected however in this annealing process, as is illustrated in figure 7(a) by a shoulder generated in the Se distri-

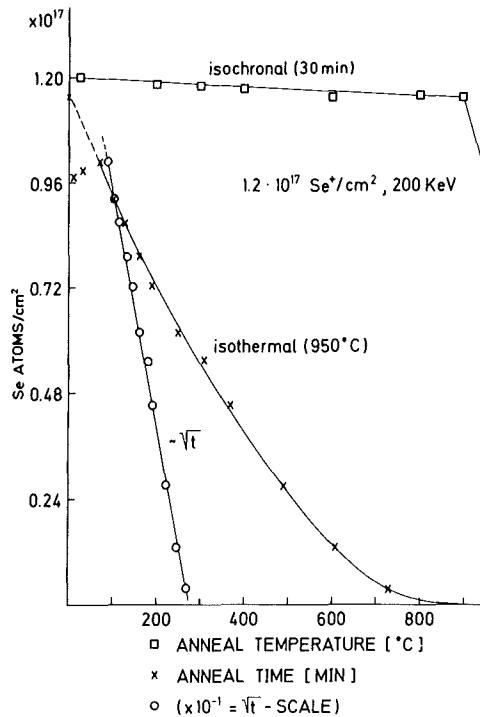


Fig. 6 Number of implanted Se atoms/cm<sup>2</sup> remaining in vanadium as a function of temperature and heating time, indicating the Se atom loss in an isothermal process at 950°C.

bution. This shoulder is thought to be caused by a fast diffusing component and its removal at about 950°C accompanies a break-up of a part of the polycrystalline layer. Isothermal annealing at 950°C revealed a selenium loss which, as can be seen from figure 6, was proportional to the square root of the annealing time. The loss process as depicted in figure 7(b) seems to have the characteristics of a diffusion from an infinitesimally thin layer into a body of finite dimensions with capturing boundaries. We believe that both diffusion processes are strongly dependent on the release of atoms from precipitations. This release from precipitations is thought to be the cause of the partial break-up of the polycrystalline layer.

Bismuth ions, with an atomic radius greater than that of vanadium, again show some specific diffusion characteristics. Isochronal annealing to 600°C produced little diffusion. Between 600°C and 1000°C however, loss of bismuth was accompanied by a deeply

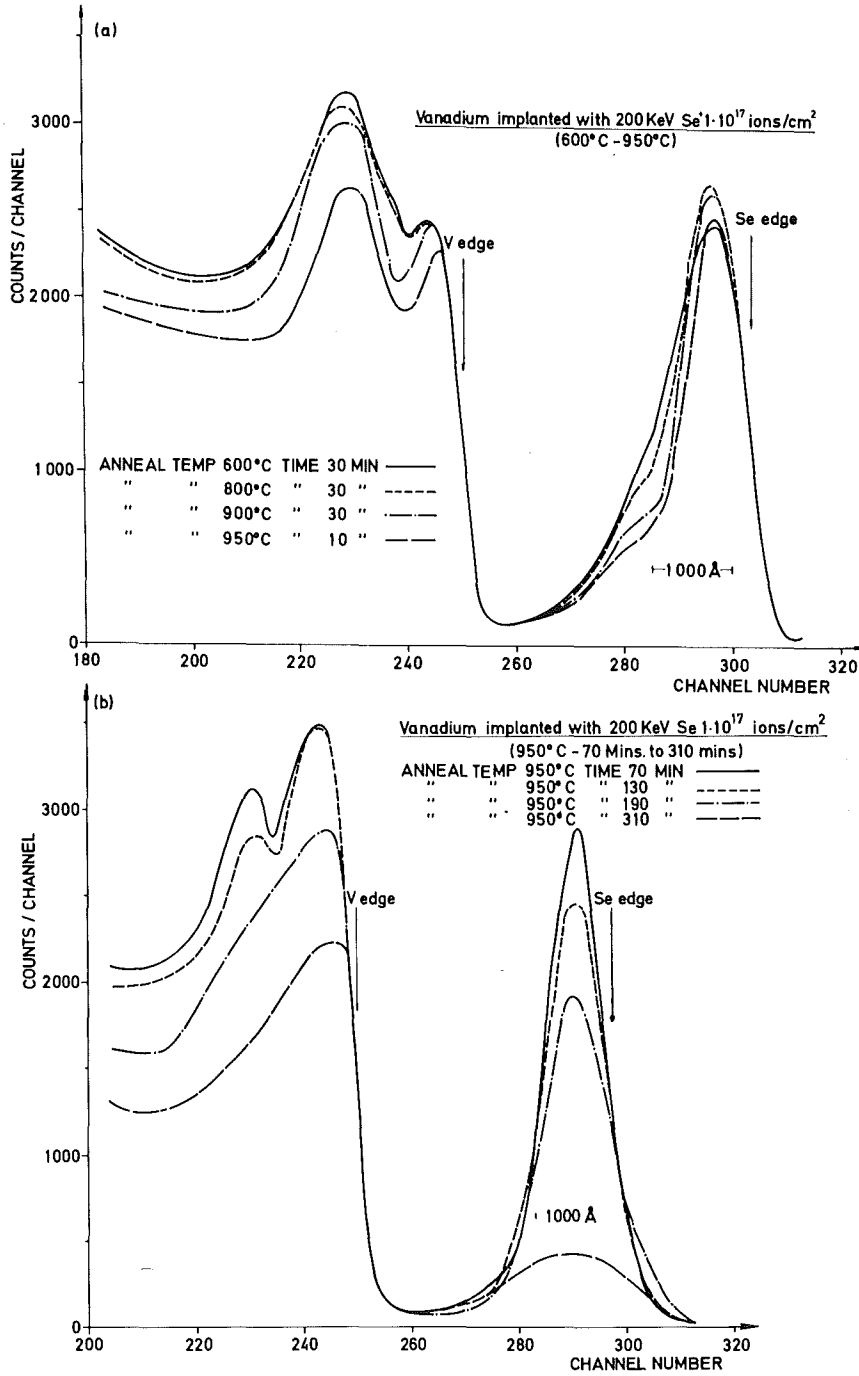


Fig.7 Se-peaks from backscattering spectra showing the two different stages in the Se diffusion process.

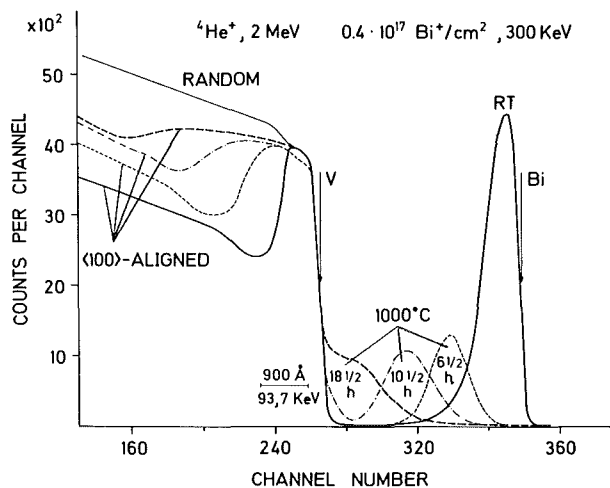


Fig. 8 Backscattering spectra from an as implanted ( $0.4 \times 10^{17}$  Bi/cm<sup>2</sup>, 300 keV) vanadium sample and from different stages in an isothermal heat treatment process at 1000°C. The main characteristics shown are an increase of the Bi distribution width and a shift of this distribution towards the vanadium edge, together with a broadening of the polycrystalline layer.

penetrating tail in this ions distribution. In an isothermal study at 1000°C, no appreciable loss of implanted ions occurred although an increase in the half width of the bismuth distribution was evident. This process is illustrated in figure 8. The apparent movement of the whole Bi distribution towards the vanadium edge in the spectra can be explained by a vanadium atom migration to form an effective thickening of the polycrystalline layer at the surface. This explanation is supported by an observed broadening of this layer in the channelled backscattering spectra. The assumed vanadium migration to the surface was not accompanied by an appreciable specimen oxidation, as the use of the helium-oxygen resonance with this sample revealed the same oxygen content as was found in freshly etched specimens.

For the Bi ions implanted in nickel a rapid loss of this constituent was observed during the annealing stage of the deep damage. In a first attempt to obtain quantitative results for diffusion processes observed in our study, experimental ion distributions were compared with theoretical distributions calculated using various

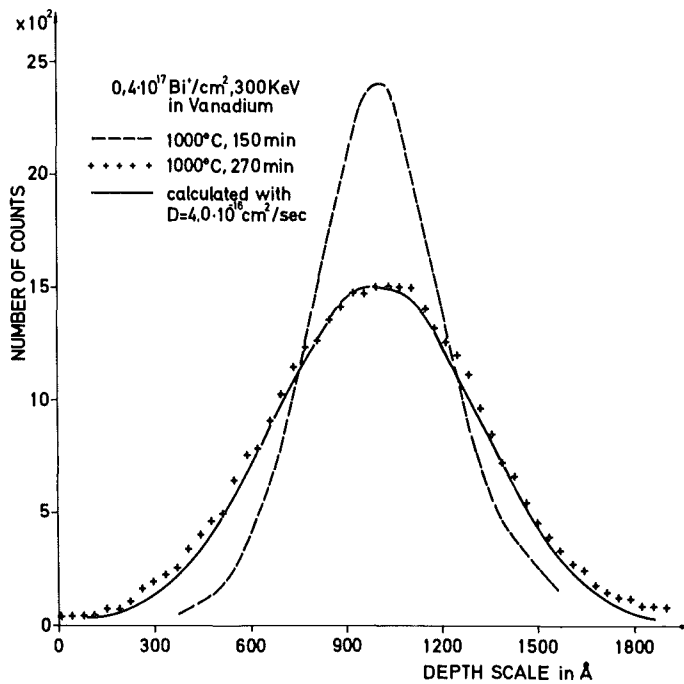


Fig. 9 Experimental and calculated Bi distributions together with the initial distribution used in the calculations.

values of the diffusion coefficient. The "best fit" for the broadening of the Bi peak at 1000°C was obtained using a diffusion coefficient of  $D = 4.0 \times 10^{-16} \text{ cm}^2/\text{sec}$ . Experimental and theoretical profiles, together with the initial distribution used in these calculations, are shown in figure 9. The solution of the diffusion equation used for this example was for diffusion from an arbitrary distribution into an infinite body.

#### CONCLUSIONS

The results of this study have shown that Bi ion implantation in both nickel and vanadium generates damage components within the ion range and at much deeper depths. We believe that the deep disorder could be due to the migration of interstitials (possibly assisted by focussed collisions) which form clusters at depths 2 to 3 times greater than the ion range. At high implantation doses, a polycrystalline layer was detected in vanadium over the range of the implanted ions and ascribed to the action of precipitates.

No such layer was detected in nickel, as the high sputtering yields were thought to prevent solubilities being exceeded.

Annealing of radiation damage in vanadium was found to be dependent on ion dose and while a very broad annealing stage was observed for low ( $< 1 \times 10^{16}$  ions/cm<sup>2</sup>) doses, no significant annealing was evident for doses where the polycrystalline layer was generated. For nickel however, little dependence of annealing on dose was found and the shallow and deep disorder components annealed between 350 - 650°C and 500 - 700°C respectively.

Characteristics of diffusion of implanted ion species were found to depend on the ion species under consideration. Gallium ions for example, because of their "good fit" in the vanadium lattice, diffused by a substitutional process while the observed Bi and Se diffusion was by an interstitial process. Diffusion mechanisms were thought to be strongly dependent on the behaviour of precipitates within the polycrystalline layer, such that break-up of this layer produced both a rapid in- and outdiffusion of implanted ion species. Preliminary quantitative results, which were observed by fitting theoretical and experimental diffusion profiles, indicate that diffusion coefficients are comparatively low.

While diffusion in vanadium was a comparatively slow process, bismuth loss in nickel was found to occur over a narrow temperature interval. Further work is at present being conducted to obtain more quantitative results on diffusion of ions implanted in both metals.

#### ACKNOWLEDGEMENTS

The authors would like to thank Dr. O. Meyer for his many valuable discussions, Mr. R. Smithey for his sample preparations and Mr. M. Kraatz for careful implantations.

#### REFERENCES

1. NORRIS, D.I.R., *Phil. Mag.* 19, 527, 653 (1969).
2. CHEN, C.W., MASTENBROEK, A., ELEN, J.D., *Rad. Eff.* 16, 127 (1972).
3. CHEN, C.W., *Phys. Stat. Sol. (a)* 16, 197 (1973).
4. DIEHL, J., DIEPERS, H., HERTEL, B., *Can. J. Phys.* 46, 647 (1968).

5. RAU, R.C., LADD, R.L., J.Nucl.Mat. 30, 297 (1969).
6. LINKER, G., GETTINGS, M., MEYER, O., III Int. Conf. on Ion Implantation in Semiconductors and other materials, Yorktown Heights Dec. 1973.
7. GETTINGS, M., MEYER, O., LINKER, G., to be published in Radiation Effects.
8. GETTINGS, M., LANGGUTH, K.G., MEYER, O., Verh. DPG 3, 367 (1973).
9. SMITH, H.J., Rad. Eff. 18, 65 (1973).

## DISCUSSION

Q: (J. A. Davies) Did you check your polycrystalline foils for preferred orientation? This might possibly be a contributing factor to the broader penetration profiles that you observe.

A: We did not check the foils for preferred orientation. But we have also performed implantations into evaporated layers with similar results. Even here for randomly oriented crystallites, channeling cannot be completely excluded. But in agreement with the experiments performed by H. J. Smith, recently published in Radiation Effects, we think that this effect is of minor importance.

Q: (H. Bernas) Referring to your observation of broadening in the Bi distributions after room temperature implantation. The characteristic channeling angles are large at these energies; we found it necessary to set up a goniometer in the implanter to reduce (yet not totally eliminate) channeling for 400 keV heavy ions in Ni or Fe. Did you check this point?

A: Our samples were fixed during implantation and in principle we cannot exclude channeling. But as we obtained similar distribution for implantations into foils, we believe that channeling is of minor importance and that the distribution broadening is mainly due to radiation enhanced diffusion.

Q: (L. C. Feldman) What is the lattice location of the implanted ions for the channeling and non-channeling case?

A: In the non-channeled case for Ni and V comparable numbers of about 50% of Bi atoms on lattice positions have been detected. The

enhanced number for channeled implants in Ni was about 70%. But this is a preliminary result and further channeled implants are necessary for confirmation. Up to now we have not performed channeled implants in V.

Q: (E. N. Kaufmann) With regard to your observation that Bi channeled in Ni shows a higher substitutional fraction than a random implant; an anomalous behavior for channeled implants in Ni has been reported before for Hf ions by Odden, Bertier, et al. It might be worthwhile to compare your result with theirs. I also would like to know below what dose of implant ions do you no longer observe the polycrystalline layer?

A: The formation of the polycrystalline layer was dependent on the implanted ion species and on dose. For example, for gallium, which has a good fit into the V lattice this layer was not observed in as-implanted samples for doses up to  $2 \times 10^{17}$  ions/cm<sup>2</sup> and appeared only on heat treatment. But for all ions under investigation, i.e., Se, Ga, In, Kr, and Cs, it can be stated that below  $5 \times 10^{15}$  ions/cm<sup>2</sup> the formation of a polycrystalline layer has not been observed.

Q: (G. Dearnaley) What was the dose rate and the beam heating on the 360 keV Bi<sup>+</sup> implantations?

A: About  $10 \mu\text{A}/\text{cm}^2$  and there would be a small amount of beam heating. The specimens were 2 mm in thickness.

PRINTED IN U.S.

ION IMPLANTATION IN SUPERCONDUCTING THIN FILMS

O. Meyer, H. Mann and E. Phrilingos

Institut für Angewandte Kernphysik

Kernforschungszentrum Karlsruhe

ABSTRACT

Selected ions were implanted at room temperature in thin films of the transition metal superconductors Ti, Zr, V, Nb, Ta, Mo, W and Re, the A-15 compound Nb<sub>3</sub>Sn and the interstitial compounds NbC and NbN with NaCl structure. Both chemically active and inert ions were used in order to distinguish between radiation damage and other effects influencing the superconducting transition temperature  $T_C$ . Successively larger decreases in  $T_C$ , due to radiation damage, were obtained for NbC, NbN, Mo, Ta, V, Nb and Nb<sub>3</sub>Sn in that order. Chemically active ions were found to produce the same reduction in  $T_C$  as inert ions in Ta, V, Nb and Nb<sub>3</sub>Sn, whereas in those materials in which radiation damage is less influential, namely NbC, NbN, Mo, W and Re,  $T_C$  enhancement was found to occur and was dose-dependent.

INTRODUCTION

The influence of radiation damage on superconducting properties of material reported so far was mainly concerned with critical current and critical field measurements<sup>(1)</sup>. Light ions were usually used (up to mass 4) and ion doses were kept below  $10^{13}$  ions/cm<sup>2</sup>. The enhancement of the critical field due to the formation of pinning centers produced during irradiation was found by several investigators to have a maximum within this dose range. Only a slight effect on the transition temperature,  $T_C$  was observed in these earlier studies.

A far higher degree of disorder than that produced by light ion irradiation can be obtained in metal films made by vapour quenching<sup>(2,3)</sup> (evaporation on a cold (4°K) substrate). Such films usually show a fine grained structure with crystallite sizes smaller than about 50 Å and in some cases a transformation into a liquid-like amorphous phase appeared to take place. In general it was observed that for vapour-quenched non transition metal films  $T_C$  is substantially higher than that of bulk material. The reason for this  $T_C$  enhancement can probably be found in the decrease of the average phonon frequency, a phenomenon that has been discussed in several theoretical treatments<sup>(6,7)</sup>. Lattice disorder also influences the electronic band structure which seems to be important for the superconducting properties in transition metals, where the bulk  $T_C$  correlates well with the electronic density of states at the Fermi edge,  $N(0)$ . In general it was found that for vapour quenched films of group V-B (V, Nb, Ta with large  $N(0)$ )  $T_C$ 's are lower than the bulk  $T_C$ 's and in vapour-quenched films of Mo, W and Re (low  $N(0)$ )  $T_C$ 's are higher than bulk  $T_C$ 's<sup>(8)</sup>. The situation in sputtered films<sup>(4)</sup> and in films produced by electron beam evaporation in a vacuum of  $10^{-5}$  -  $10^{-6}$  Torr<sup>(5)</sup> is further complicated, as it has been shown that metastable high  $T_C$  phases can be stabilized by impurities, structural defects and intrinsic stresses.

The purpose of the present work was to investigate the influence of disorder and impurities produced by heavy ion bombardment on the superconducting properties. Ion implantation has been used to introduce damage and impurities in a controlled manner into solids. The effect of radiation damage on  $T_C$  can be separated from the effects of the incorporated impurities by either using inert gas ions or by implanting through the metal layer so that the ions come to rest in the substrate. Chemical effects on  $T_C$  have been studied by implanting ions of different solubilities in the host lattice. Additional information has been obtained by studying radiation damage and solubility levels in ion implanted vanadium single crystals using transmission-electron-microscopy and the backscattering and channelling technique<sup>(9)</sup>.

#### EXPERIMENTAL AND ANALYSIS

Films of the transition metals Ti, Zr, V, Nb, Ta, Mo, W and Re together with  $Nb_3Sn$  with thicknesses from 100 to 4000 Å, were prepared by electron beam evaporation and by co-deposition onto quartz substrates in an ultra-high vacuum system where a pressure of 1 to  $5 \times 10^{-8}$  Torr could be maintained during evaporation. The bakeable UHV-system consists of a turbomolecular pump, an ion getter pump and a titanium evaporation pump. NbN layers have been produced by reactive sputtering in an argon-nitrogen plasma. During the production of NbC layers in an argon-plasma the Nb-target

has been covered by a perforated carbon plate<sup>(10)</sup>

These films were implanted with selected ions from every group of the periodic system. Ion energies used were in the range 50 to 400 keV, and doses were from  $10^{14}$  to  $10^{17}$  ions/cm<sup>2</sup>. Dose rates were maintained between 0.1 and 10  $\mu$ A/cm<sup>2</sup>. Layer thickness, sputtering during implantation, and the depth distribution of implanted ions were recorded by use of the nuclear backscattering technique. The usefulness of this technique is demonstrated in Fig. 1 where the backscattering spectra, obtained with 2 MeV  $\alpha$ -particles from a Mo layer are shown prior to and after implantation of  $1 \times 10^{17}$  S<sup>+</sup>/cm<sup>2</sup> at 130 keV. By analysis of such spectra, which is described elsewhere<sup>(11)</sup>, one can obtain the sputter yield (here about 3). By additional thickness measurements of the Mo-layer and the step between implanted and unimplanted Mo-layer, as indicated in Fig. 1, density changes in the implanted layer can be determined.

The superconducting transitions were measured resistively, with  $T_C$  being defined as the temperature at which the resistance decreased to half of its normal value. During implantation the layers were partially covered in order to restrict the implanted area to  $(5 \times 10)$ mm<sup>2</sup>. For the  $T_C$  measurements the voltage contacts (Fig. 2) were placed at equal distances from the boundary between the implanted and unimplanted areas. With this contact arrangement the resistance drop reveals a step as it is shown in Fig. 2 for V and Nb layers implanted with N<sup>+</sup> ions at various doses. For comparison the resistance drop of the unimplanted layer is included. The resistance curves of the implanted layers show two steps. The first step coincides with the resistance drop of the unimplanted layer, which can be used as a check to show that the shielded part of the layer is not influenced during the implantation procedure. The difference  $\delta T_C$  between the onset of the transition in the unimplanted layer and the temperature where the implanted layer was found to be completely superconducting was used as a measure of the damage influence on  $T_C$ . In the case where  $T_C$  enhancement is observed the results were confirmed by placing the voltage contacts directly onto the implanted layer. Diffraction patterns have been taken with a thin film X-ray camera in order to see if ion implantation has any effect on grain size and film structure.

## RESULTS

Layers with the following  $T_C$ 's have been routinely produced: Ti, Zr, Mo and W with  $T_C < 1.2^\circ\text{K}$ ; V ( $4.5 - 5.3^\circ\text{K}$ ), Nb ( $8.3 - 9.3^\circ\text{K}$ ), Ta ( $4 - 4.45^\circ\text{K}$ ), Re ( $1.5 - 1.7^\circ\text{K}$ ), Nb<sub>3</sub>Sn ( $18.2^\circ\text{K}$ ), NbN ( $15 - 16^\circ\text{K}$ ), NbC ( $9 - 11^\circ\text{K}$ ). The width of the transitions were usually  $< 0.1^\circ\text{K}$ .

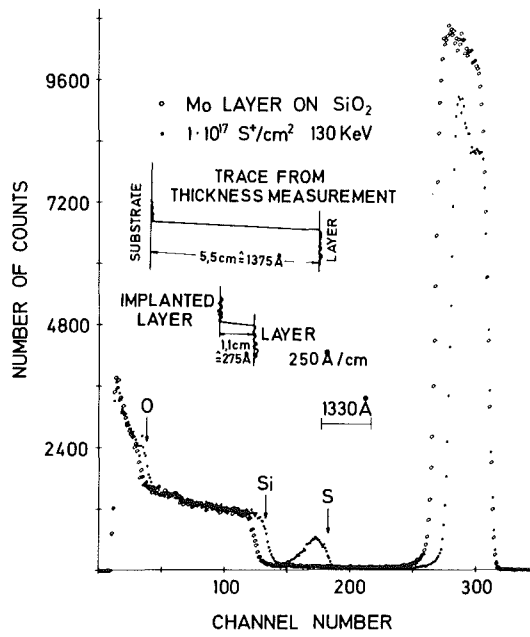


Fig. 1 Backscattering spectra obtained from an implanted and unimplanted part of a Mo layer. Together with thickness measurements, shown in the inset, the sputter yield and the density change in the implanted layer is determined.

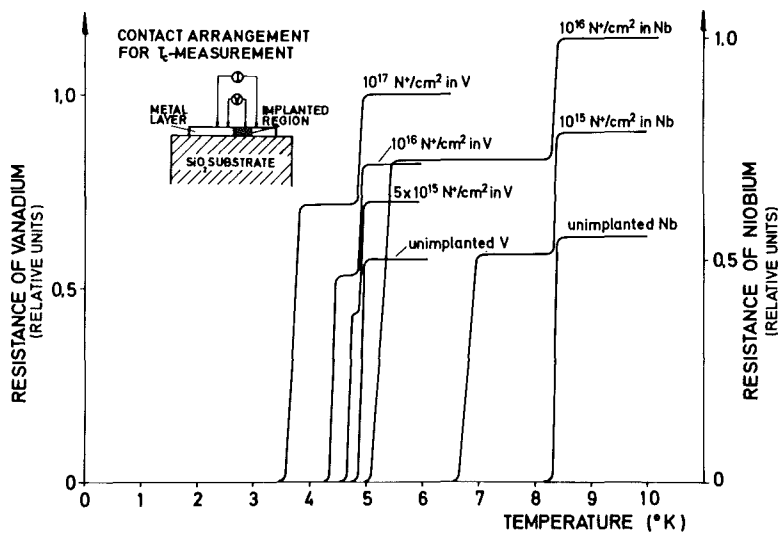


Fig. 2 Resistance versus temperature for Nb and V thin films, implanted with low energy  $\text{N}^+$  ions at different doses. The inset shows the contact arrangement.

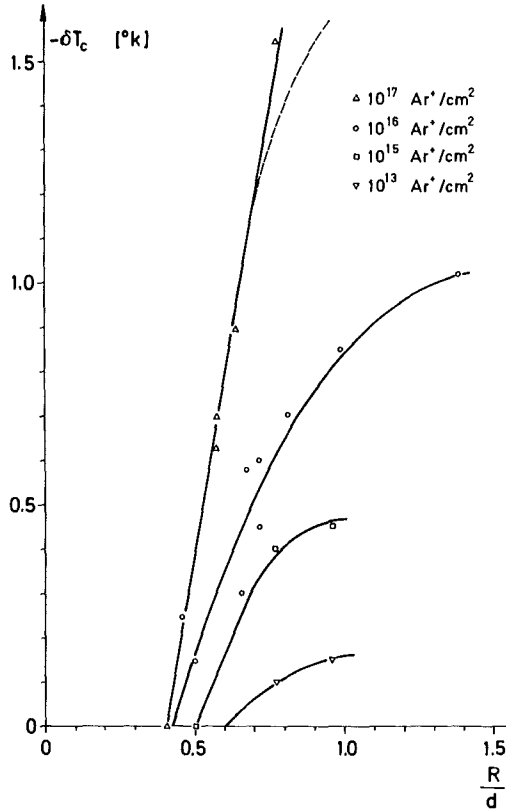


Fig. 3. Decrease in  $T_C$  for V versus the ratio  $R/d$  with the ion dose as parameter.

a) Influence of Radiation Damage on  $T_C$  in V.

In order to study the influence of radiation damage on  $T_C$ , the metal films were implanted with the chemically inert Ar<sup>+</sup> and Kr<sup>+</sup> ions. The magnitude of the decrease in  $T_C$ ,  $\delta T_C$ , was found to depend on the range of the implanted ions. This dependence is shown in Fig. 3 for Ar<sup>+</sup> ions implanted in V at four different doses. The observed  $\delta T_C$  is plotted as a function of the ratio  $R/d$  where quantity  $d$  is the layer thickness and  $R = R_p + 1.17 \Delta R_p$ . Here  $R_p$  and  $\Delta R_p$  are the mean projected range and the range straggling, respectively, as determined from the LSS theory<sup>(12)</sup>. It can be seen that  $\delta T_C$  has a saturation level for  $R/d \geq 1$ . In further experiments

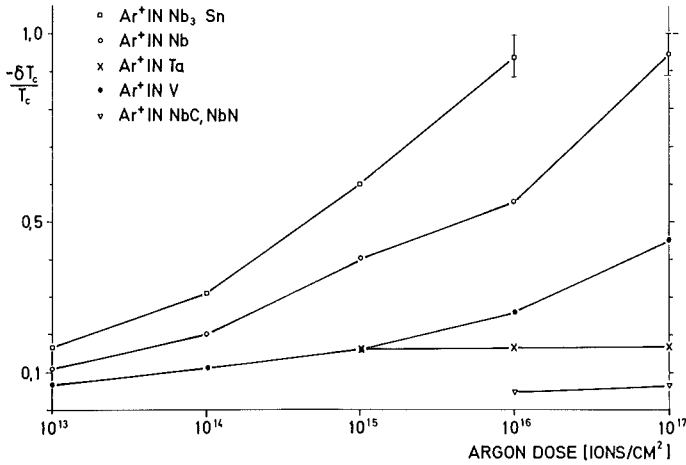


Fig. 4  
Decrease in  $T_C$ , normalized to the bulk  $T_C$ , versus ion dose for different superconducting materials.

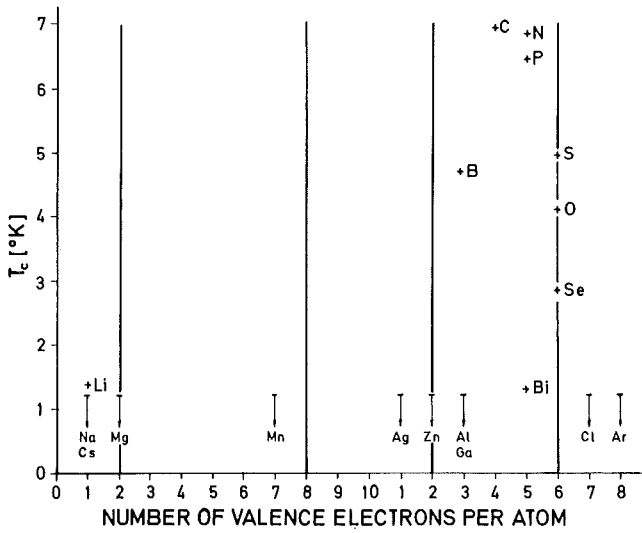


Fig. 5  
 $T_C$  enhancement in Mo after implanting ions with various numbers of valence electrons per atom.

where  $R$  exceeds  $d$  by a factor 3 to 4 it has been verified that the decrease in  $T_C$  is due to the damage produced and not due to incorporated noble gas ions. The observed decrease in  $T_C$  for  $R/d < 1$  is probably due to enhanced defect diffusion during implantation. If this were not the case the undamaged region of the metal layer would provide an effective short circuit. Defects deeper than  $R_p$  have also been found in ion implanted V single crystals by use of channelling technique and transmission electron microscopy<sup>(9)</sup>. In all further damage experiments  $R/d$  was kept about 1 by suitable choice of ion energy.

The influence of damage on  $T_C$  in different materials is sum-

marized in Fig. 4 where  $\delta T_C$ , normalized to the corresponding  $T_C$  of the bulk material is presented as a function of argon ion dose. The effect of damage on the  $T_C$  of  $Nb_3Sn$  layers was found to be stronger than that observed in V and Nb. For example by the implantation of  $10^{16} Ar^+/cm^2$  the initial  $T_C$  of 17.8°K was decreased to 2.0°K. For a constant dose it can be seen that  $\delta T_C/T_C$  increases for material with increasing electronic density of states at the Fermi edge. Vanadium is an exception as  $N(O)_V > N(O)_{Nb}$ . NbC and NbN are found to be highly radiation resistant. No effects on  $T_C$  were observed by bombardment with protons and  $He^+$  ions at doses up to  $10^{16}$  ions/cm<sup>2</sup> which is in agreement with results presented in (1). A possible impurity effect due to the implanted ions has been further investigated by implanting  $Ga^+$  ions in V and Nb. By comparison of  $\delta T_C$  values for  $Kr^+$  implantation with those for  $Ga^+$  implantation, no additional effect could be detected (within the limits of our measurement errors) with up to about 20 at % of Ga atoms incorporated in V and Nb films.

Since grain size is not affected by ion implantation as was verified by thin film X-ray diffraction and since resistivity measurements show the mean free path of electrons at  $T > T_C$  is not strongly reduced, it is assumed that the smearing out of structure in the electronic density of states is not the only factor in the decrease of  $T_C$  by radiation damage. If this were true there should also occur an increase in  $T_C$  for argon implanted Mo due to damage, but this is not observed.

#### b) Chemical Effects of Implanted Ions

Possible chemical effects were studied by implanting ions from nearly all groups of the periodic system in those transition metals where the damage effect is presumably low, i.e. where  $N(E)$  has no sharp peaks at the Fermi edge. In Fig. 5 the  $T_C$  enhancement observed by implanting ions with various values of valence electrons per atom in Mo layers is summarized.  $T_C$  enhancement up to 7°K was observed for implantation of elements from groups III(B), IV(C), V (N, P, Bi) and VI (S, O, Se).

For elements which are completely insoluble in Mo no  $T_C$  enhancement is observed. Those elements which form stable intermetallic compounds, either superconducting or non-superconducting, give  $T_C$  enhancement. It is possible that the elements that tend to form intermetallic compounds stabilize the disorder in Mo on a microscopic scale, thereby producing the  $T_C$  enhancement. Preliminary results also show enhancement of  $T_C$  by implantation of  $N^+$  and  $S^+$  ions in W and Re. A summary of the results obtained by ion implantation,  $T_C^{II}$ , in transition metals is given in TABLE I and are compared with the bulk value  $T_C^{Bulk}$ , theoretical values for amorphous transition metals (14)  $T_C^{Theory}$ ,  $T_C^{VQ}$  for vapor-quenched films (8) and  $T_C^{SP}$  for "reactively"

Metal	$T_C^{\text{Bulk}}$	$T_C^{\text{Theory}}$ (VQ)	$T_C^{\text{VQ}}$	$T_C^{\text{SP}}$	$T_C^{\text{II}}$
Ti	0.39	0.5	-	-	$\leq 1.2$
Zr	0.5	0.1-0.5	3.5	0	$\leq 1.2$
V	5.3	9	-	$\leq 5.3$	2-3
Nb	9.2	7.4-8.2	6	$\leq 9.2$	3-5
Ta	4.5	2.7-3.5	2	$\leq 4.3$	3-4
Mo	0.9	9.6	8.5	7-8	$\sim 7$
W	0.01	4-4.3	3.5	$\sim 4$	$\sim 3.5$
Re	1.7	6.2-7.5	7.5	$\sim 7$	$\sim 4.5$

Table I  
Experimental (ion implantation, vapour-quenching, sputtering) and theoretical results for  $T_C$  of some transition metals.

sputtered films (<sup>5,17</sup>). As the values of  $T_C^{\text{II}}$  are strongly dose dependent, maximum values were given for  $T_C$  enhancement, whereas for the  $T_C$  decrease the values obtained for  $10^{16}$   $\text{Ar}^+/\text{cm}^2$  have been used.

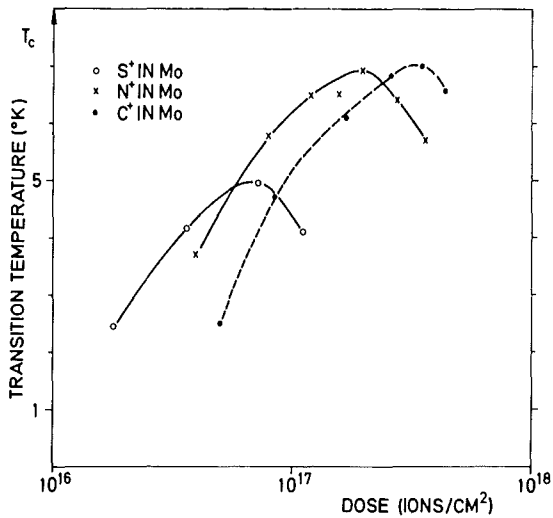


Fig. 6  
Dose dependence of  $T_C$  enhancement after implanting  $\text{S}^+$ ,  $\text{N}^+$  and  $\text{C}^+$  ions in Mo.

No increase in  $T_C$  was found after implanting ions with low solubilities in Ti and Zr, whereas after implanting  $\text{Fe}^+$  ions in Ti a  $T_C$  of about  $3^\circ\text{K}$  has been observed. This increase in  $T_C$  is probably due to the increase of the number of electrons per atom by implanting soluble elements, an effect which will be studied

further in more detail. Preliminary results on non transition metals (Al, Sn) show that implanting  $B^+$  and  $S^+$  increased the  $T_C$  of Al to  $2.5^{\circ}K$  and of Sn to  $4.4^{\circ}K$ . Only a slight increase of about  $0.1^{\circ}K$  has been observed by implanting  $Ar^+$  ions in Al under similar conditions. The dose dependence of the  $T_C$  enhancement is presented in Fig. 6 for  $S^+$ ,  $C^+$  and  $N^+$  ions implanted in Mo. A maximum value in  $T_C$  is observed.  $T_C^{max}$  increases with decreasing mass of implanted ions and shifts to higher doses. These maxima were found to occur for lower ion doses in Re and for higher doses in W as compared with the results presented for Mo. More detailed studies especially on the density changes in the implanted layers

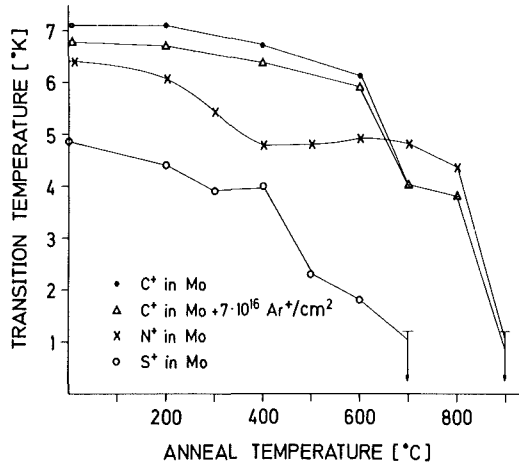


Fig. 7  
Influence of an isochronal anneal process on  $T_C$  of implanted Mo layers.

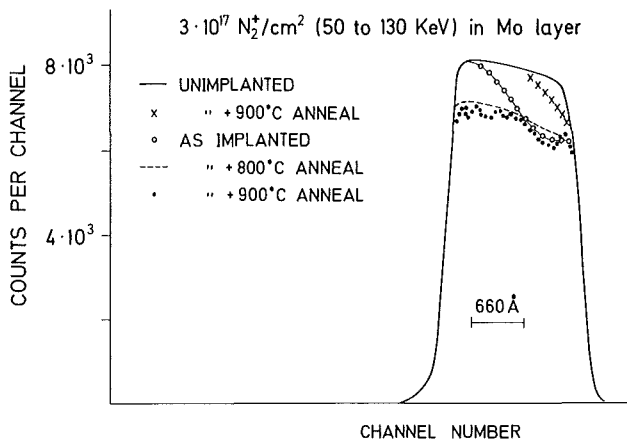


Fig. 8  
Backscattering spectra from implanted and unimplanted Mo layers at room temperature and at  $800^{\circ}C$  and  $900^{\circ}C$ .

are necessary and will be done in the future.

### c) Annealing Effects

Isochronal annealing processes in a vacuum of  $10^{-7}$  Torr have been performed on implanted Mo layers and the dependence of  $T_C$  on annealing temperature is shown in Fig. 7. The  $T_C$  enhancement is found to be stable for annealing temperatures up to  $400^\circ\text{C}$  in  $S^+$  implanted layers and up to  $800^\circ\text{C}$  in  $C^+$  and  $N^+$  implanted layers. The influence of lattice disorder was studied by additional implanting  $7 \times 10^{16} \text{ Ar}^+/\text{cm}^2$  in a  $C^+$  implanted Mo layer with a  $T_C$  of  $7.2^\circ\text{K}$ . The observed  $T_C$  reduction of  $0.5^\circ\text{K}$  as shown in Fig. 7 is small compared to results presented in Fig. 4. From the backscattering spectra taken from implanted Mo layers and unimplanted layers it can be seen (Fig. 8) that at  $800^\circ\text{C}$  the nitrogen has moved through-out the metal layer. At  $900^\circ\text{C}$  additional oxygen has been incorporated as can be seen in the spectra of the unimplanted layer and the inhomogeneities visible in the spectra of the implanted layer seem to indicate the formation of precipitations. The increase of  $T_C$  due to  $V_3\text{Si}$  formation<sup>(13)</sup> has prevented study of the effect of anneal temperature on implanted V layers. In the case of the  $\text{Nb}_3\text{Sn}$  films, however, the influence on  $T_C$  due to radiation damage has been found to be removed on annealing for several hours at  $800^\circ\text{C}$ .

### DISCUSSION

To summarize, we found a strong decrease of the transition temperature of Ta, V, Nb, and  $\text{Nb}_3\text{Sn}$  films after bombarding with low energy high mass ions. The magnitude of the decrease in  $T_C$  was found to depend on mass, dose and range of implanted ions, and is therefore attributed to the radiation damage produced during implantation and not to chemical effects. It is assumed that the smearing out of structures in the electronic state density distribution is only one reason for the observed decrease in  $T_C$ . Otherwise, argon implantation in W, Mo and Re should produce a  $T_C$  increase for the same reason, but this is not observed. The disturbance of the long range order in  $\text{Nb}_3\text{Sn}$  may explain the strong decrease of  $T_C$  found for that material.

$T_C$  enhancement was observed by implanting selected ions able to form intermetallic compounds but otherwise of low solubility in Mo, W, and Re films. It is assumed that these ions do not stabilize a high  $T_C$  phase after implantation but can stabilize a dislocation of the lattice atoms. The suggestion that implantation of impurities will stabilize high  $T_C$  phases largely composed of the element in question, as was observed in transition metal films evaporated in a vacuum of  $10^{-5}$  to  $10^{-6}$  Torr<sup>(4)</sup> or sputtered in the presence of gaseous impurities<sup>(5)</sup>, can be discussed as follows:  
In contrast to results given in<sup>(4)</sup> our layers had bulk  $T_C$ 's in

the limit of measurement ( $T_C \geq 1.2^\circ\text{K}$ ). X-ray patterns of unimplanted Nb and Mo films did only show the normal bcc phase. The implanted regions of these layers did not show any difference in the X-ray pattern. There was no evidence for the presence of other phases and there was no spread in the line width indicating small grain sizes. In addition the implanted Mo layers with high  $T_C$  were stable against irradiation with argon ions and stable against temperature treatment. In forming an impurity stabilized high  $T_C$ -phase one would also expect a saturation in the dose dependence of  $T_C$  rather than a maximum.

There are several arguments against the suggestion that the high  $T_C$  phases of MoN and MoC have formed during implantation. Firstly, the dose for maximum  $T_C$  enhancement was lower than necessary for the formation of stoichiometric MoN and MoC, secondly  $N^+$  in W increased  $T_C$  but no high  $T_C$  WN-phase is known.  $N^+$  in Ti and Zr did not increase  $T_C$  but TiN as well as ZrN are known to be superconducting.

The stabilized dislocation mentioned above may change the atomic volume<sup>(14)</sup> and therefore the electron density which causes a shift in the density of states at the Fermi edge. A further possible reason for this shift may be found in the high electronegativity of the implanted ions causing a  $T_C$  increase. The observed maxima in the dose dependence of  $T_C$  and the shift in the maxima for different material may be explained with the assumption that the Fermi energy is shifted across a peak in  $N(E)$  resulting in a maximum in  $T_C$ . The observed increase or decrease in  $T_C$  may also be discussed in terms of the Eliashberg function  $\alpha^2(w) F(w)$ <sup>(15)</sup> which describes the interaction between phonons and electrons causing the effective attraction between the electrons in a superconductor. It has been shown for nontransition metals<sup>(16)</sup> that the softening of the phonon distribution and therefore of  $\alpha^2 F(w)$ , in highly disordered superconductors can result in either a positive or a negative change in the transition temperature. In this regard the observed decrease in  $T_C$  for the group Vb elements may be due to a decrease in  $\alpha$  or due to a shift of  $F(w)$  to higher frequencies.

Further, by implanting ions of higher solubility in the host lattice it is possible to change the number of electrons per atom and to increase  $T_C$  in suitable ion - target systems.

#### ACKNOWLEDGEMENT

Thanks are due to M. Kraatz and R. Smithey for careful layer preparation and ion implantation and to F. Ratzel for performing  $T_C$  measurements. We further want to thank W. Buckel, J. Geerk, M. Gettings and G. Linker for many helpful discussions.

## REFERENCES

- (1) G.W. CULLEN in BNL-50155 (1968) p. 437.
- (2) W. BUCKEL and R.J. HILSCH, Z. Phys. 132, 420 (1952); 138, 109 (1954).
- (3) Review of M. STRONGIN Physica Vol. 55, 155 (1971).
- (4) W.L. BOND et al., Phys. Rev. Lett. 15, 260 (1965).
- (5) K.L. CHOPRA, M.R. RANDLETT, and R.H. DUFF, Phil. mag. 16, 261 (1971).
- (6) R.C. DYNES, Solid State Communications, 10, 615 (1972).
- (7) J.W. GARLAND, K.H. BENNEMANN and F.M. MUELLER, Phys. Rev. Letters 21, 1315 (1968).
- (8) M.M. COLLVER, R.H. HAMMOND, Phys. Rev. Letters 30,92 (1973).
- (9) M. GETTINGS, G. LINKER and O. MEYER, III. Int. Conf. on Ion Implantation, New York, Dec. 11-14, 1972.
- (10) O. MEYER, G. LINKER and B. KRAEFT, Int. Conf. on Ion Beam Surface Layer Analysis, Yorktown Heights, New York, June 18-20, (1973).
- (11) G. LINKER, O. MEYER and M. GETTINGS, Int. Conf. on Ion Beam Surface Layer Analysis. Yorktown Heights, New York, June 18-20, (1973).
- (12) J. LINDHARD, H.E. SCHIØTT, and M. SCHARFF, Mat. Phys. Med. 33 2 (1963).
- (13) F.J. CADIEU, in AIT Conf. Proc. No. 4, 213 (1972), ed. by D.H. Douglass.
- (14) K.H. BENNEMANN, Winter Colloquium in Schleching 19.2-23.2. (1973).
- (15) J.R. SCHRIEFFER, Theory of Superconductivity, Benjamin Inc. Publ. N.Y. 1964.
- (16) G. BERGMANN and D. RAINER, Z. Physik 263, 59 (1973).
- (17) D. GERSTENBERG, P.M. HALL, J. Electrochem. Soc. 111, 936 (1964).